ORIGINAL PAPER

Characterization of fresh and aged natural ingredients used in historical ointments by molecular spectroscopic techniques: IR, Raman and fluorescence

L. Brambilla · C. Riedo · C. Baraldi · A. Nevin ·
M. C. Gamberini · C. D'Andrea · O. Chiantore ·
S. Goidanich · L. Toniolo

Abstract Natural organic materials used to prepare pharmaceutical mixtures including ointments and balsams have been characterized by a combined non-destructive spectroscopic analytical approach. Three classes of materials which include vegetable oils (olive, almond and palm tree), gums (Arabic and Tragacanth) and beeswax are considered in this study according to their widespread use reported in ancient recipes. Micro-FTIR, micro-Raman and fluorescence spectroscopies have been applied to fresh and mildly thermally aged samples. Vibrational characterization of these organic compounds is reported together with tabulated frequencies, highlighting all spectral features and changes in spectra which occur following artificial aging. Synchronous fluorescence spectroscopy has been shown to be particularly useful for the assessment of changes in oils after aging; spectral difference between Tragacanth and Arabic gum could be due to variations in origin and processing of raw materials. Analysis of these materials using non-destructive spectroscopic techniques provided important analytical information which could be used to guide further study.

Keywords Oils · Gums · Beeswax · FTIR · Raman · Fluorescence · Non-destructive analysis

Published in the special issue *Analytical Chemistry to Illuminate the Past* with guest editor Maria Perla Colombini.

L. Brambilla (✉) · S. Goidanich · L. Toniolo
Department CMIC, Politecnico di Milano,
via Mancinelli 7,
20133 Milano, Italy
e-mail: laura.brambilla@chem.polimi.it

C. Riedo · O. Chiantore
Department of IPM Chemistry and NIS-Centre of Excellence,
University of Turin,
10124 Turin, Italy

C. Baraldi · M. C. Gamberini
Department of Pharmaceutical Sciences, Institute of Pharmacy,
University of Modena and Reggio Emilia,
via G. Campi 183,
41125 Modena, Italy

A. Nevin · C. D'Andrea
Department of Physics, Politecnico di Milano,
Piazza L. da Vinci 32,
20133 Milano, Italy

Introduction

Since antiquity, natural organic materials from animals and plants have been used in the formulation of pharmaceutical mixtures. Organic materials have been routinely used in the preparation of unguents and balsams and are described in medical and cosmetic recipes [1]; a study of treatises and research into the identification and aging behavior of ingredients used in preparations are part of the project entitled "Colors and balms in antiquity: from the chemical study to the knowledge of technologies in cosmetics, painting and medicine (CiBA)". The investigation of historical samples of balsams and unguents—coming from containers in archaeological sites, museum or pharmaceutical collections [2] represents a significant analytical challenge because the aged materials are complex mixtures of organic and inorganic ingredients, they may be contaminated and are often heavily degraded and we lack sufficient spectroscopic databases of raw materials for the analytical recognition of samples.

In the framework of the CiBA project, a large collection of ancient recipes has been assembled, and representative raw materials used in the past for different preparations have been tabulated. In this work, the principal organic ingredients used in historical preparations have been analyzed and include: vegetable oils (olive, almond and palm tree), gums (Arabic and Tragacanth) and beeswax. The selected materials, and in particular the three oils are relatively rarely encountered in the analysis of cultural heritage and paintings where drying oils are more commonly investigated [3–5]. Olive oil has been widely studied by Fourier transform infrared (FTIR) and Raman spectroscopy in agricultural and food science [6, 7]; most recently, investigations have focussed on the geographical origin [8] and potential adulteration of the precious oil [9]. Almond oil has only rarely been studied, in contrast to palm oil, as it is rarely used for food [10]. Natural gums are vegetal exudates of tropical trees and plants and are water soluble or dispersible polysaccharides of high molecular weight [11]; these materials are well known as binders in paint, the principal medium for watercolors, and a common ingredient in paint used in manuscript illumination [12, 13]. However, today gums are principally used as an emulsifier in food and pharmaceutical industries [11, 14]. Wax, and mainly that from bees, has been used in preparations since antiquity. Beeswax is particularly well known as an adhesive, surface coating, painting medium and as a modeling and casting material and contains hydrocarbons, free acid and esters. The mid-infrared and Raman characterization of beeswax has been carried out and published in well-established studies [15–17]. This group of well-known natural materials has been generally characterized by chromatographic techniques (GC-MS/PY-MS/HPLC) requiring relatively large samples and pre-treatment procedures; this approach can guarantee a thorough detection of the different components of the material, but sample treatment and extraction indeed becomes critical in the analysis of complex mixture of many ingredients.

This work, therefore, aims to characterize different primary materials before and after artificial aging using molecular spectroscopic methods. Mild thermal aging has been applied to samples because, in museum and collection storage, the vessels are generally kept closed in dark conditions. Three different analytical techniques—micro-FTIR spectroscopy, micro-Raman spectroscopy and fluorescence spectroscopy—have been applied as synergic instruments for the characterization of the raw materials. The specific aim of this approach is to determine the best results which can be obtained using each technique on reference samples and to provide attributed reference spectroscopic data for future studies. The main advantage in this approach is that it utilizes non-destructive and micro-destructive techniques which can be extended to the analysis of historical micro-samples which may be hardly visible to the naked eye.

Materials and methods

Olive oil was supplied by a farmer (Sicily, Italy), almond oil by Marco Viti Officina di Mozzate (Como, Italy) and palm oil is a common commercial product. Arabic and Tragacanth gums were supplied by Sigma-Aldrich. Beeswax was supplied by a farmer (Pisa, Italy). About 0.5 g of oils and beeswax have been applied in thin layers in glass Petri dishes while gums have been swollen in distilled water and cast as thin films on glass slides. Each material has been studied before and after artificial aging. Mild thermal aging consists of 1,000 h of oven heating at 60 ± 5 °C. The samples have been analyzed after different aging times (0, 24, 120, 168, 312, 360, 500, 624, 816 and 1,000 h).

Micro-FTIR spectroscopy

Infrared spectroscopy was carried out on micro-samples using a compression diamond cell by Thermo Scientific and a Continuum microscope coupled with a Nicolet 6700 spectrophotmeter (Thermo Scientific)—spectral range between 4,000 and 650 cm^{-1}, with 4 cm^{-1} resolution. Oils and beeswax have been spread directly on the diamond cell surface, without any treatment. Gums have been dissolved in water, cast on glass slides and left to dry at room temperature; a very small fragment of the gum film was placed on the diamond cell surface for FTIR analysis.

Raman spectroscopy

FT-Raman spectra were recorded by using a Bruker Multi-ram spectrometer, equipped with a FRA 106 FT-Raman module and with a near IR continuous-wave Nd/YAG laser operating at 1,064 nm in backscattering. The laser was focused on an area of 100×100 μm of the sample and a liquid nitrogen-cooled germanium detector was used. Approximately 2,000 scans with a resolution of 4 cm^{-1} were averaged for each sample. Maximum power on the sample was 15 mW.

Fluorescence spesctroscopy

A Jobin Yvon Fluorolog Spectrofluorimeter equipped with a Xenon lamp, double excitation monochromators and a single emission monochromator was employed for analysis of raw materials. All materials were analyzed as films (cast either from solutions of gums, from melted

wax or directly from a drop of oil prior to and following aging) on quartz disks and were analyzed in front face (23°) geometry. This geometry has been shown to be most suitable for the collection of fluorescence from the surface of scattering media and is particularly useful for the analysis of trace fluorophores in bulk materials including edible oils [18]. A suitable sample holder was constructed for the positioning of the quartz disks during analysis. Slits were fixed to 1 nm for the excitation monochromators and 5 nm for the emission monochromator. Excitation, emission and synchronous fluorescence spectra (with an offset between the exciation and emission monochromators) were recorded for the different materials. Maxima in fluorescence bands are given as excitation wavelength (in nm)/emission wavelength (in nm).

Results and discussion

The main results obtained are described in the following sections according to the different classes of materials: oils, beeswax and vegetal gums.

Oils

Vibrational spectroscopy

In Table 1, the attribution of bands in spectra of fresh and aged oils is reported. It can be noticed that while FTIR spectroscopy is not able to distinguish between fresh olive and almond oil, Raman spectroscopy suggests some differences between the two oils. The major observed difference is the presence of the band at 1,266 cm^{-1} in almond oil

Table 1 FTIR and Raman wave numbers and assignments for fresh and aged oils [20]

FTIR (peak position (cm^{-1}))						RAMAN (peak position (cm^{-1}))						Vibrational mode
Fresh			Aged			Fresh			Aged			
Olive	Almond	Palm	Olive	Almond	Palm	Olive	Almond	Palm	Olive	Almond	Palm	
			3,483	3,479	3,487							ν_{OH}
3,005	3,007	3,006				3,008	3,007 w	3,006				$\nu_{sC=C-H}$ (cis)
2,956 sh	2,954 sh	2,955										ν_{asCH_3}
2,925	2,926	2,925	2,927	2,928	2,925	2,923 sh	2,923 sh	2,923 sh	2,921	2,927 vs, broad	2,927 sh	ν_{asCH_2}
						2,897	2,900	2,880			2,880	ν_{asCH_3}
2,854	2,855	2,854	2,855	2,856	2,854	2,853	2,850 vs	2,850	2,854	2,854 vs	2,853	ν_{asCH_2}
1,747	1,747	1,747	1,743	1,743	1,744	1,749	1,749 w	1,746	1,742	1,742 w	1,742	$\nu_{C=O}$ ester
	1,712				1,712							$\nu_{C=O}$ fatty acid
									1,670	1,674 vw		$\nu_{C=C}$ (trans)
						1,656	1,658 vs	1,654			1,657	$\nu_{C=C}$ fatty acids (cis)
									1,636	1,637 vw	1,633	$\nu_{C=C}$ fatty acids
								1,523				$\nu_{C=C}$ carotenoids
1,464	1,465	1,465	1,464	1,464	1,465		1,457 m, sh	1,453	1,456	1,457 sh	1,458	δ_{asCH_3}
						1,441	1,439 s	1,440	1,441	1,443 vs	1,441	δ_{CH_2} scissoring
1,418	1,417	1,418	1,415	1,418	1,418							ν_{C-O}
1,378	1,378	1,378	1,378	1,377	1,378							δ_{sCH_3}
						1,304	1,305 m	1,296	1,306	1,307 s	1,298	τ_{ipCH_2}
							1,266 m	1,268				$\delta_{ip=C-H}$ (cis)
1,240	1,236	1,239	1,244	1,239	1,239							ν_{C-O}
1,164	1,164	1,165	1,169	1,170	1,168							ν_{C-O}
								1,156				ν_{C-C} carotenoids
1,096	1,096	1,098	1,099	1,095	1,097	1,088	1,085 mw	1,084	1,083	1,085 m	1,082	ν_{C-O}
						1,066	1,066 w	1,064	1,068	1,064 m	1,064	ν_{C-C}
								1,004				ν_{C-C} carotenoids
			978	972	973							$\delta_{C=C-H}$ (trans)
									873	880 m very broad	890+870 sh	ρ_{CH_2}
723	723	722	726	725	723							$\delta_{C=C-H}$ (cis)

ν stretching, δ bending, ρ rocking, τ twisting

which corresponds to the rocking vibration of C–H (symmetric rocking in *cis* double bond). Other differences are seen at 1,439 cm^{-1} (methylene scissoring) and 1,658 cm^{-1} (*cis* double-bond stretching), for which the peak intensities are completely inverted in almond oil with respect to the same bands in olive oil. For palm oil, the FTIR spectrum of the fresh sample shows a splitting of the $\nu_{C=O}$ peak in a doublet at 1,712 and 1,747 cm^{-1} due to the presence of ester and free acid functional groups of carboxylic fatty acid. This spectral feature is characteristic of aged drying oils including linseed oil [5]. In the Raman spectrum of palm oil, the presence of β-carotene bands at 1,525 (conjugated C=C stretching), 1,156 and 1,004 cm^{-1} (stretching of skeletal C–C) can be easily noted and used as distinctive features. In the spectral range of 3,006–2,854 cm^{-1}, the spectra of all three oils are similar.

Vibrational spectroscopies can distinguish between fresh and aged samples due to key spectral differences (see Table 1 and Fig. 1). The main changes observed in Raman and FTIR spectra during the aging process can be summarized as follows: disappearance of *cis*-C=C–H stretching peak at 3,007 cm^{-1}; broadening and shift of the –C=O asymmetric stretching peak, more evident in Raman (from 1,749 to 1,742 cm^{-1}) than in FTIR (from 1,747 to 1,743 cm^{-1}) spectra. This last phenomenon can be ascribed to the formation of major secondary oxidation products (e.g. aldehydes).

Raman spectroscopy suggests other spectral differences following thermal aging: (a) formation of a band at about 1,674 cm^{-1}, which could be assigned to *trans*-C=C double bonds [19]; (b) appearance of a band at 1,635–1,637 cm^{-1}, which could be assigned to the stretching of conjugated dienes; (c) disappearance of νC=C of fatty acids at 1,658 cm^{-1} and of the symmetric rocking of C–H in-plane deformation at 1,266 cm^{-1}; (d) increase of the peaks due to –CH$_2$ scissoring at 1,440 cm^{-1} and to –(CH$_2$)$_n$ chain deformations at 1,307–1,297 cm^{-1}, depending on the different oils considered; and (e) appearance of a band at 880 cm^{-1} probably due to –CH$_2$ and –CH$_3$ rocking that can be considered characteristic of thermal aged oils. An examination of Raman spectra suggests the scission of the carbon chain at double bonds; in fact, methyl terminal rocking exhibits a broader band in the range of 975–835 cm^{-1} for $n<10$ [20]. In the case of thermally aged palm oil, Raman spectra confirm the complete loss of β-carotene.

In Fig. 1, FTIR spectra of almond oil acquired at different times of thermal aging are reported, as an example. In addition to the spectral differences mentioned above, during aging other changes are observed and include: (a) the appearance of a broad band ascribed to O–H stretching cantered at 3,479 cm^{-1}; (b) the appearance of *trans*-C=C–H band at 972 cm^{-1}; and (c) intensity reduction of the bending peak around 723 cm^{-1} and the disappearance of the peak at 3,007 cm^{-1} which are both ascribed to the *cis*-C=C–H [5]. The simultaneous occurrence of the described changing suggests that the *cis* double bonds are isomerized to *trans* configuration. Such changes are observed for all three oils during aging. The time required for the observing the first aging features is shorter for almond oil, followed by olive oil and palm oil, which is the most resistant to thermal aging. During the aging the intensity of carbonyl asymmetric stretching peaks increases while that of −CH$_2$ decreases significantly, both for olive and almond oil. Peak area determination, before and after 1,000 h of thermal aging, allows the quantification of intensity changes. The ratio of the peak area νCH$_2$/νC=O was evaluated for all the three fresh and aged oils and is reported in Fig. 2. The ratio νCH$_2$/νC=O is 1.9 for fresh

Fig. 1 FTIR spectra of almond oil during thermal aging in three characteristic spectral ranges (3,760–2,500, 1,915–1,580 and 1,045–580 cm^{-1}). Spectra have been plotted with a fixed offset from one another and peaks which change significantly with aging have been indicated with an arrow and labeled
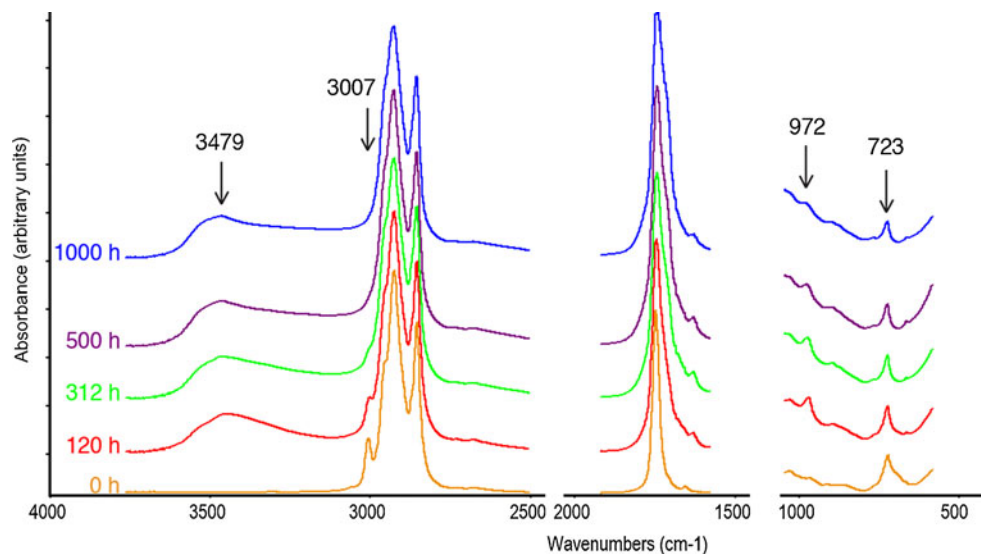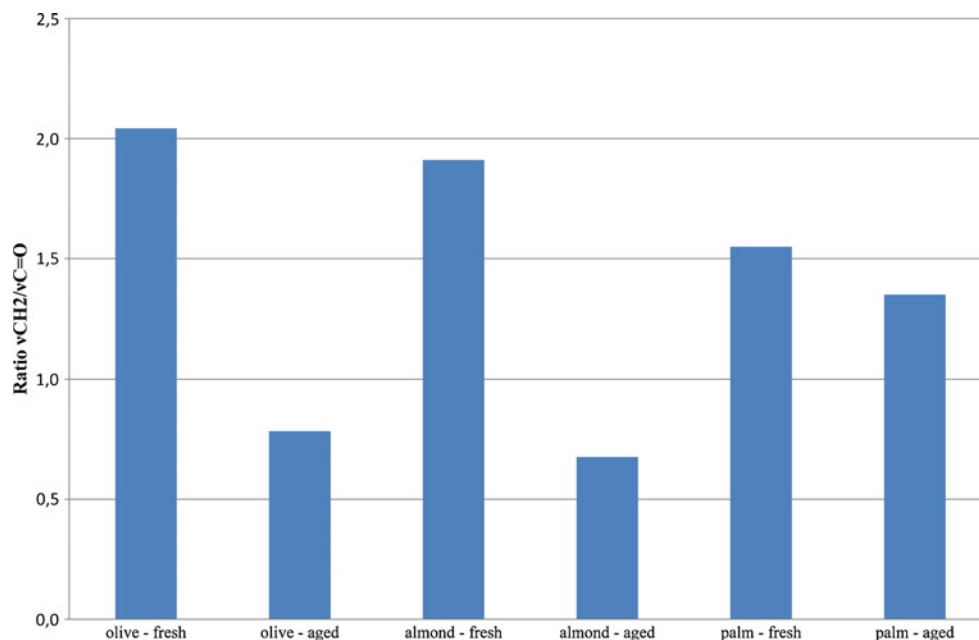
Fig. 2 νCH$_2$/νC=O peak area ratio for olive, almond and palm oil

almond oil and 2.0 for fresh olive oil; 0.7 for aged almond oil and 0.8 for aged olive oil. It is worth noting that results from FTIR confirm that palm oil is more resistant to aging, considering that the same ratio is changes from 1.5 for fresh oil to 1.3 for aged oil. For reference, FTIR and Raman spectra recorded from un-aged and artificially aged palm oil have been provided in the Electronic Supplementary Material.

Electronic spectroscopy

The fluorescence of natural oils (which are a mixture of fatty acids and other trace molecules) is well known and has been extensively studied [18, 21–23]. The edible oils analyzed in this work are all characterized by a strong fluorescence band with excitation in the range between 270 and 310 nm and emission in the range from 300 to 350 nm, ascribed to tocopherols [21], and multivariate models for the determination of tocopherol concentration as a function of fluorescence have been proposed [18]. In the visible range, emissions from carotenoids at 673 nm (palm oil) [22] and chlorophyll at 405/670 nm (olive oil) [23].

Fluorescence spectroscopy has been employed to assess the mild thermal oxidation which occurs as a result of the artificial aging of oils. The accumulation of oxidation products in all oils was accompanied by a marked yellowing (of olive and almond oil) with aging, and all oils are sticky and thicker than the un-aged materials. Polymerization and oxidation also lead to a significantly more complex mixture of compounds in the artificially aged materials and significant changes in the fluorescence properties of the oils [18, 23–25]. Particularly evident is an increase in the emission in the visible range, which can be attributed to a range of oxidation products [24] and the total loss of chlorophyll emissions at 670 nm. Synchronous fluorescence (SF) spectroscopy has been shown to be useful for the assessment of change in edible oils [23] due to the fact that information from a range of different excitation and excitation wavelengths is contained within a single spectrum [18]. For analysis of aged oils in this work, SF has been employed at an offset of 60 nm, which has been shown to be sensitive to changes as a result of oxidation of olive oil [23] (Fig. 3).

The artificial aging of the oils examined in this work induces a marked increase in visible fluorescence (here seen as a wide emission band centered at approximately 425 nm). A similar trend has been documented in the analysis of other oils during aging and thermal oxidation at higher temperatures [24] or during storage [26]. Bands centered at excitation/emission of 350/450 nm are related to the formation of hydroperoxides [27, 28]. The band at around 330 nm in all three oils is associated with tocopherols (prior to and following aging), and this band does not significantly change in shape upon aging, which suggest that isomerization of tocopherols, reported for aging of oils [29] does not influence the position of the emission at 330 nm. In addition, results suggest that aging at moderate conditions (60 °C) does not lead to the more extensive molecular changes, and consequent loss of fluorescence from tocopherols as has been shown for oils heated about 190 °C [24]. Both olive oil and almond oil have similar fluorescence spectra following aging which is in contrast to aged palm oil, which presents a wider emission band
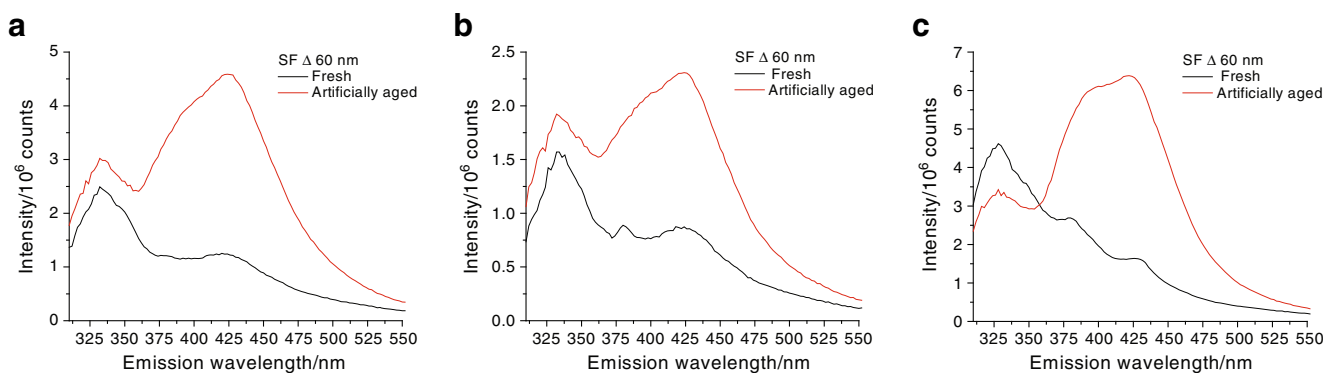
Fig. 3 Synchronous fluorescence spectra of fresh and artificially aged (**a**) almond oil, (**b**) olive oil and (**c**) palm oil with an offset of 60 nm between excitation and emission monochromators

with a distinct shoulder at 400 nm. This difference in fluorescence behavior could be related to the prooxidative effect attributed to the caretenoids in palm oil [26] and a build up of trace tocopherol degradation products [29] and in trace fatty acid oxidation products [25].

Beeswax

Vibrational spectroscopy

Beeswax is a complicated mixture in which fatty acids and aliphatic esters of animal origin can be easily detected using vibrational spectroscopy. It consists mainly of esters of fatty acids with high molecular weight alcohols, the corresponding free fatty acids and monohydric alcohols and *n*-alkanes [30].

Both FTIR and Raman spectra of beeswax show the typical CH_2 peaks of hydrocarbons in the 2,960–2,840 and 1,473–1,377 cm^{-1} regions. In the Raman spectrum characteristic, CH_2 twisting is found at 1,299 cm^{-1}. The well-known asymmetric $\nu C=O$ of esters and corresponding free acid, are detected in FTIR spectra at 1,736 and 1,712 cm^{-1}. The intense and broad band at 1,174 cm^{-1} relative to the $\nu C–O$ vibration of esters is present in both spectra. In the Raman spectrum bands at 1,134 cm^{-1} ($\nu C–C$ and νCOC vibrations) and 1,065 cm^{-1} ($\nu C–C$ vibrations) are also observed [15, 16].

The very intense IR absorption bands at 730 and 720 cm^{-1} are the marker peaks due to in-plane rotation of linear long carbon chains ($\delta(CH_2)_n$) [17, 30]. This doublet is diagnostic of the presence of beeswax also in very complex mixture, as far as it appears in a generally not crowded spectral region. The Raman spectrum in the same region shows a weak peak at 892 cm^{-1}. After aging, no spectral changes have been detected in beeswax due to the saturated nature of the hydrocarbon chains which provide the well-known stability of waxes [30].

Electronic spectroscopy

The fluorescence of beeswax is well known; in contrast to the study of natural oils, the fluorophores present in the complex material have received little attention. In addition, due to the highly scattering microcrystalline solid wax, diffuse reflectance is a significant complication for the recording of emission spectra. Scattering phenomena indeed dominate emission spectra recorded using lamp-based sources, and these effects can be minimised by recording spectra with monochromatic laser excitation. Indeed, fluorescence spectra of beeswax have been published with laser excitation at 337 and a broad emission at 400 nm [31]; at 351.1 nm excitation, in addition to the emission observed at 400, another band centered at approximately 550 nm was recorded in cooled films of wax (25 K) [32], which is similar to the peak reported at 520 nm and also associated with beeswax [33].

In this work, SF spectra of films of beeswax were recorded. The SF spectrum of beeswax acquired with an offset of 60 nm has two distinct bands (see Fig. 4 and Table 2), but it is not possible to ascribe the bands to
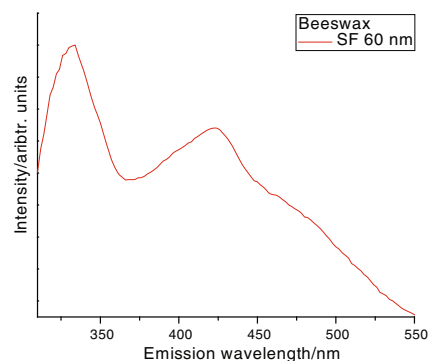

Fig. 4 Synchronous fluorescence spectrum of beeswax with an offset of 60 nm between excitation and emission monochromators

Table 2 Maxima in synchronous fluorescence spectra recorded at 60 nm offset for raw materials with a suggested attribution based on chromophores reported in the literature [14, 24, 27, 28, 36], full width at half maximum (FWHM)

Material	Emission wavelength (nm)/ FWHM	Suggested attributions
Olive, almond and palm oil	332/50	Phenolic compounds and hydroxyperoxides
	424/100	tocopherols
Gum Arabic and gum Tragacanth	334/30	Tryptophan, Maillard reaction products
	382/65	and phenolic compounds
	412 (shoulder)	
Beeswax	334/55	Unidentified phenolic, cinnamic acids
	424	and flavonoid compounds
	452 (shoulder)	

specific molecules. Flavonoids and cinnamic acids (associated with an emission at 420 nm [24]) have been identified in beeswax using complementary destructive analyses [30, 34], and it is therefore hypothesized that these molecules and their precursors may be responsible for the strong fluorescence which is observed in films of the material.

Gums

Vibrational spectroscopy

In Table 3, the attribution of bands in vibrational spectra of gums is reported. Only limited FTIR data have been published regarding plant gums and no precise vibrational characterization have been published while Raman spectroscopy of gums has been more thoroughly investigated [15, 35] Gums are complex mixtures of saccharides [12], arabinose, rhamnose, galactose, glucose, etc. and uronic acids (precisely galacturonic and glucuronic acids), together with vegetal proteins (polypeptides) and this complex composition complicates the interpretation of vibrational spectra. The relative amount of the different components changes according to the different exudates and provenance [12, 36].

In the FTIR spectrum of fresh analyzed samples, the peak at 3,420 cm^{-1} is ascribed to the asymmetric stretching of O–H group of polysaccharides and the wide peak at 2,932 cm^{-1} to the stretching vibrations of CH$_2$ groups, present in the different chemical environments. In the Raman spectrum the complex and broad feature centered at 2,930 cm^{-1} is similarly due to aliphatic C–H stretching.

In the region between 2,000 and 850 cm^{-1} (Fig. 5), the two gums show some differences in FTIR spectra: the presence of the strong peak at 1,750 cm^{-1} due to the C=O asymmetric stretching of galacturonic acid [36] is detected for the tragacanth sample. Between 1,640 and 1,610 cm^{-1}, the symmetric stretching of the carboxylate group is generally observed (–COO$^-$), together with the same vibration for –OH groups. In the case of tragacanth gum the FTIR peak is well centered at 1,639 cm^{-1} indicating the prevalent presence of salted –COOH functional groups; in

the case of Arabic gum a distinct doublet can be easily observed. This situation has been pointed out by Renard [36] for different molecular fractions analyzed in the characterization of Acacia gum from Senegal, the spectrum of which is roughly similar to that of gum Arabic. With Raman spectroscopy, instead, in the region 1,600–1,750 cm^{-1} only very weak bands are visible and can be attributed to carboxylic acid νC=O features. Other notable FTIR patterns are the two intense peaks at 1,100 and 1,018 cm^{-1}, connected to the presence of uronic acid [37], clearly visible in the spectrum of Tragacanth gum. Finally, the asymmetric stretching of C–O–C ether group of the ring at 1,075 and 1,078 cm^{-1}, for Arabic and Tragacanth, respectively, is a very distinctive feature. In the same region, between 1,050 and 1,100 cm^{-1}, the Raman spectrum shows the νCC modes, whereas νCOC ring mode and glycosidic bonds between sugar residues are visible between 800 and 950 cm^{-1} (doublets 882–844 cm^{-1} for Arabic sample and 940–866 cm^{-1} for Tragacanth) [15, 35]. In the FTIR absorption at 978 cm^{-1}—a shoulder in the Tragacanth sample—can be ascribed to the methyl substitution of the carboxylate group [36]. The same peak, although of low intensity, is visible in the Raman spectrum of Arabic gum but is absent in Tragacanth.

In the FTIR spectra collected after 1,000 h of thermal aging (not shown), no differences have been detected in absorption band distribution, showing that the major components of plant gums are stable to thermoxidation in the monitored exposure time.

Electronic spectroscopy

Emission spectra of gum Arabic and gum Tragacanth have been published with laser excitation at 363.8 nm which give rise to broad bands with a maximum at approximately 450 nm [32], but the origin of the emission in both gums was not ascribed. Both gum Arabic and gum Tragacanth are heteropolysaccharides containing between 2% and 3% polypeptides, and it is amino acids which give rise to the strong fluorescence detected in the UV (Fig. 6). Molecular fractions of the aqueous polypeptide extracts of gum Arabic

Table 3 FTIR and Raman wave numbers and assignments for gums [15, 35–37]

FTIR (peak position (cm^{-1}))		RAMAN (peak position (cm^{-1}))		Vibrational mode
Gum Arabic	Gum Tragacanth	Gum Arabic	Gum Tragacanth	
3,424	3,424			ν_{OH}
2,932	2,935	2,942	2,936	ν_{CH_2} (asym)
	1,751			$\nu_{C=O \; uronic \; acid}$
1,635	1,639			ν_{COO}
1,612				
	1,443	1,459	1,459	$\delta_{CH_2 \, scissoring}$
1,424	1,426			δ_{CH_2}
1,385	1,375		1,377	δ_{CH_3}
	1,333	1,343	1,342	$\delta_{CH_2 \, wagg.}$
1,312				$\delta_{CH_2 \, ester}$
1,290				$\delta_{CH_2 \, ester}$
1,261		1,261	1,267	τ_{CH_2}
1,233	1,246			δ_{CH_2}
1,143	1,152		1,146	ν_{CC}
			1,128	ν_{CC}
	1,100 sh		1,107	$\nu_{CC \; uronic \; acid}$
1,075	1,078	1,078	1,082	$\nu_{COC \; ether \; group \; (ring)}$
1,037	1,033			ν_{CC}
	1,020		1,020	$\nu_{CC \; uronic \; acid}$
979	978 sh	978		ρ_{CH_3}
			940	ν_{COC}
		882		ν_{COC}
			866	ν_{COC}
		844		ν_{COC}
			770	ν_{CC}
		716	719	ν_{CC}
		623	621	δ_{CCC}
		568	572	δ_{CCO}
		542		δ_{CCO}
		482	478	δ_{CCC}
		459	442	δ_{CCC}
		352	366	τ_{CCC}

ν stretching, δ bending, ρ rocking, τ twisting

Fig. 5 Normalized spectra of Arabic gum (*black*), Tragacanth gum (*green*), in the spectral region 1,950–850 cm^{-1}
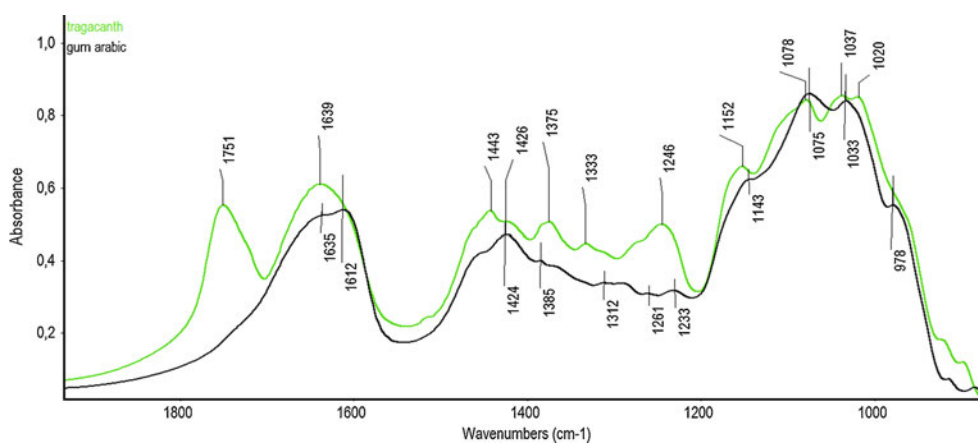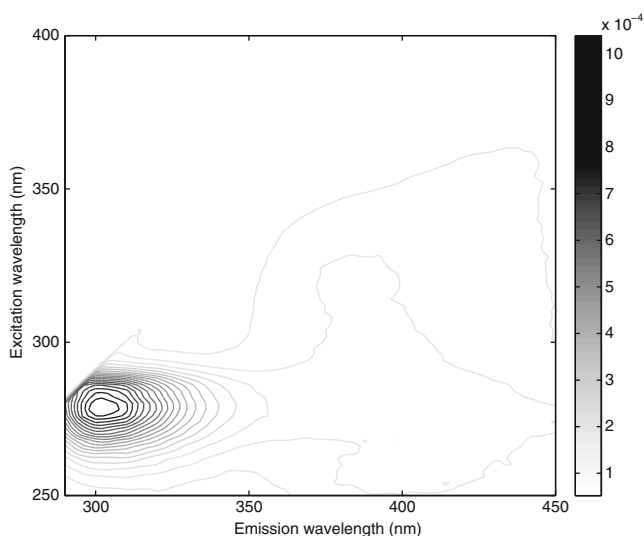
Fig. 6 Fluorescence excitation emission spectrum of a film of gum Arabic

have been shown to contain both Tyr and Phe (from GC-MS analysis) and Trp from UV–vis absorption [36]. While fluorescence ascribed to Trp (290:342–45) was observed in isolated fractions of the gum, no signal from Trp was observed in solutions of the bulk material. Additional fluorescence in the isolated molecular fractions of the material have been reported with an emission maximum centered at 413–415 nm which has been ascribed to phenolic compounds including caffeic and ferulic acid (with maxima at 330:425 and 330:415) [36].

The fluorescence excitation emission spectrum of a film of gum Arabic (and gum Tragacanth, not shown) has a strong band with a maximum at 278:302 nm (full width at half maximum, 50 nm). The band is ascribed to emissions from Tyr, identified in both gums [36, 38] and minor

contributions from Tryptophan which give rise to the broadening of the emission. SF spectra of both gums (shown in Fig. 7) highlight the emission from Trp. At an offset of 25 nm, SF spectra are dominated by a narrow band from Tyr. At an offset of 60 nm, spectral bands reflect contributions ascribed to Trp (at emissions of 335 nm), Maillard reaction products (at 375–400 nm) [14]; a slight shoulder at approximately 415 nm which is observed in gum Arabic could be related to trace phenolic compounds [36]. The spectral difference between Tragacanth and gum Arabic could be due to variations in origin and processing of the gums.

Conclusions

Spectroscopic techniques are very useful in highlighting molecular patterns characteristic of different classes of organic materials used for the preparation of cosmetics and unguents: at the same time FTIR, Raman and fluorescence spectroscopy may be able to detect chemical changes in raw materials as a function of aging processes. The synergic and contemporary use of the three considered spectroscopies is possible thanks to the low amount of sample required, the quick preparation and rapidity of analysis. The coupling of FTIR and Raman spectroscopies in this work is efficient in distinguishing among very similar oils, but, it should be noted that in real samples constituted by a mixture of different similar materials, some of the distinctive spectral features could be hidden or not visible. Spectrofluorimetry applied for the analysis of the same materials was able to detect molecular changes due to aging processes which are followed by FTIR and Raman, and the greatest changes are observed in vegetable oils following artificial thermal aging. The complete character-
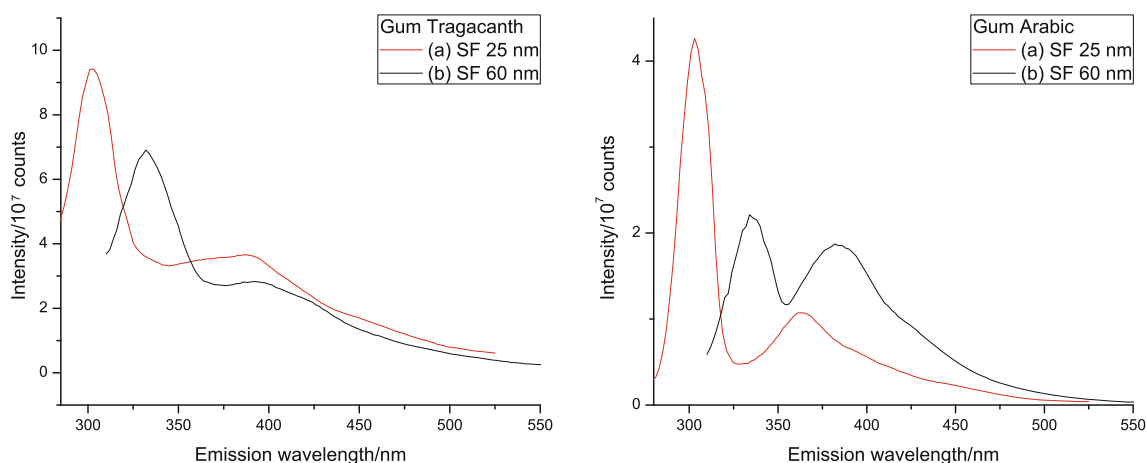

Fig. 7 Synchronous fluorescence spectra recorded from films of gum Arabic and gum Tragacanth shown at two different offsets between excitation and emission monochromators (**a**) 25 and (**b**) 60 nm

ization of the three different types of natural organic materials, with tabulated results, will be a useful guide for future analysis of archaeological samples.

References

1. Tsoucaris G, Lipkowski J (ed) (2002) Molecular and Structural Archaeology: Cosmetic and therapeutic Chemicals. NATO Sci Ser 117

2. Gamberini MC, Baraldi C, Freguglia G, Baraldi P (2011) Spectral analysis of pharmaceutical formulations prepared according to ancient recipes in comparison with old museum remains. In this volume

3. Pilc J, White R (1995) The application of FTIR-microscopy to the analysis of paint binders in easel paintings. Natl Gallery Tech Bull 16:73–84

4. Casadio F, Toniolo L (2001) The analysis of polychrome works of art: 40 years of infrared spectroscopic investigations. J Cult Herit 2:71–78

5. Van der Weerd J, Van Loon A, Boon J (2005) FTIR studies of the effects of pigments on the ageing of oil. Stud Conserv 50:3–22

6. Dahlberg DB, Lee SM, Wenger SJ, Vargo JA (1997) Classification of vegetable oils by FT-IR. Appl Spectrosc 51:1118–1124

7. Yang H, Irudayaraya J, Paradkar MM (2005) Discriminant analysis of edible oils and fats by FTIR, FT-NIR and FT-Raman spectroscopy. Food Chem 93:25–32

8. Tapp HS, Defernez M, Kemsley EK (2003) FTIR spectroscopy and multivariate analysis can distinguish the geographic origin of extra virgin olive oils. J Agric Food Chem 51:6110–6115

9. Lerma-Garcia MJ, Ramis-Ramos G, Herrero-Martinez JM, Simò-Alfonso EF (2010) Autentication of extra virgin olive oils by Fourier-transform infrared spectroscopy. Food Chem 118:78–83

10. Che Man YB, Moh MH, Van de Voort FR (1999) Determination of free fatty acids in crude palm oil and refined-bleached-deodorized palm olein using Fourier transform infrared spectroscopy. J Am Oil Chem Soc 76(4):485–490

11. Mills J, White R (1994) The organic chemistry of museum objects. Butterworth-Heinemann, Oxford

12. Bonaduce I, Brecoulaki H, Colombini MP, Lluveras A, Restivo V, Ribechini E (2007) Gas chromatographic–mass spectrometric characterization of plant gums in samples from painted works of art. J Chromatogr A 1175:275–282

13. Riedo C, Scalarone D, Chiantore O (2010) Advances in identification of plant gums in cultural heritage by thermally assisted hydrolysis and methylation. Anal Bioanal Chem 396 (4):1559–1569

14. Kuan YH, Bhat R, Senan C, Williams PA, Karim A (2009) Effects of Ultraviolet irradiation on the physicochemical and functional properties of gum Arabic. J Agric Food Chem 57:9154–9159

15. Edwards HGM, Farwell DW, Daffner L (1996) Fourier-transform Raman spectroscopic study of natural waxes and resins. I Spectrochim Acta A 52:1639–1648

16. Vandenabeele P, Wehling B, Moens L, Edwards H, De Reu M, Van Hooydonk G (2000) Analysis with micro-Raman spectroscopy of natural organic binding media and varnishes used in art. Anal Chim Acta 407:261–274

17. Campanella L, Chicco F, Colapietro M, Gatta T, Gregori E, Panfili M, Russo MV (2005) Characterization of wax manufactures of historical and artistic interest. Ann Chim 95:167–176

18. Sikorska E, Gliszczyńska-Świgło A, Khmelinskii IV, Sikorski M (2005) Synchronous fluorescence spectroscopy of edible vegetable oils. Quantification of tocopherols. J Agric Food Chem 53(18):6988–6994

19. Sadeghi-Jorabchi H, Wilson RH, Belton PS, Edwards-Webb JD, Coxon DT (1991) Quantitative analysis of oils and fats by FT Raman spectroscopy. Spectrochim Acta 47:1449–1458

20. Lin-Vien D (1991) The handbook of infrared and raman characteristic frequencies of organic molecules. Academic, New York

21. Sikorska E, Romaniuk A, Khmelinskii IV, Herance R, Bourdelande JL, Sikorski M, Koziol J (2004) Characterization of edible oils using total luminescence spectroscopy. J Fluoresc 14 (1):25–35

22. Tan YA, Chong CL, Low KS (1995) Relationship between laser-induced fluorescence intensity and crude palm oil quality. J Sci Food Agric 67:375–379

23. Sikorska E, Khmelinskii IV, Sikorski M, Caponio F, Bilancia MT, Pasqualone A, Gomes T (2008) Fluorescence spectroscopy in monitoring of extra virgin olive oil during storage. Int J Food Sci Technol 43:52–61

24. Tena N, García-González DL, Aparicio R (2009) Evaluation of virgin olive oil thermal deterioration by fluorescence spectroscopy. J Agric Food Chem 57:10505–11051

25. Guimet F, Ferré J, Boqué R, Vidal M, Garcia J (2005) Excitation–emission fluorescence spectroscopy combined with three-way methods of analysis as a complementary technique for olive oil characterization. J Agric Food Chem 53:9319–9328

26. Yi J, Anderson ML, Skibsted LH (2011) Interactions between tocopherols, tocotrienols and carotenoids during autoxidation of mixed palm olein and fish oil. Food Chem 127:1792–1797

27. Kyriakidis NB, Skarkalis P (2000) Fluorescence spectra measurement of olive oil and other vegetable oils. J Am Oil Chem Soc 83 (6):1435–1439

28. Cheikhausma R, Zude M, Bouveresse DJR, Rutledge DN, Birlouez-Aragon I (2004) Fluorescence spectroscopy for monitoring extra virgin olive oil deterioration upon heating. Czech J Food Sci 22:147–150

29. Verleyen T, Kamal-Eldin A, Dobarganes C, Verhe R, Dewettinck K, Huyghebaert A (2001) Modeling of alpha-tocopherol loss and oxidation products formed during thermoxidation in triolein and tripalmitin mixtures. Lipids 36(7):719–726

30. Regert M, Colinart S, Degrand L, Decavallas O (2001) Chemical alteration and use of beeswax through time: accelerated ageing tests and analysis of archaeological samples from various environmental contexts. Archaeometry 43(4):549–569

31. Miyoshi T (1987) Fluorescence from varnishes for oil paintings under N_2 laser excitation. Jpn J Appl Phys 26:780–781

32. Larson LJ, Shin KSK, Zink JI (1991) Photoluminescence spectroscopy of natural resins and organic binding media of paintings. J Amer Inst Conserv 30(1):89–104

33. Comelli D, Valentini G, Cubeddu R, Toniolo L (2005) Fluorescence lifetime imaging and fourier transform infrared spectroscopy of Michelangelo's David. Appl Spectrosc 59 (9):1171–1181

34. Tomás-Barberán FA, Ferreres F, Tomás-Lorente F, Ortiz A (1993) Flavonoids from *Apis mellifera* beeswax. Z für Naturforschung 48C:68–72

35. Edwards HGM, Falk MJ, Sibley MG, Alvarez-Benedi J, Rull F (1998) FT-Raman spectroscopy of gums of technological significance. Spectrochim Acta A 54:903–920

36. Renard D, Lavenant-Gourgeon L, Ralet MC, Sanchez C (2006) Acacia senegal gum: continuum of molecular species differing by their protein to sugar ratio, molecular weight and charges. Biomacromol 7:2637–2649

37. Coimbra MA, Barros A, Barros M, Rutledge DN, Delgadillo I (1998) Multivariate analysis of uronic acid and neutral sugars in whole pectic samples by FT-IR spectroscopy. Carbohydr Polym 37:241–248

38. Anderson DMW, Bridgeman MME (1985) The composition of the proteinaceous polysaccharides exuded by *Astragalus microcephalus*, *A. gummifer* and *A. kurdicus*—the sources of Turkish Gum Tragacanth. Phytochemistry 24(10):2301–2304